

Structural Verification of a Fiberglass/Polyimide Acoustic Inlet for the DC-10

William R. Dunbar*

Douglas Aircraft Company, McDonnell Douglas Corporation, Long Beach, Calif.

A program was undertaken to determine the structural suitability of a composite acoustic inlet for the DC-10 wing engine. Airframe and mission structural requirements for the inlet were determined. A flightworthy prototype panel was designed, fabricated, and tested. Mechanical properties were determined in the laboratory. The general durability and resistance to sonic fatigue were determined by over 250 hr of combined ground and flight testing in front of a CF6 engine. Blade fragment penetration resistance tests were conducted.

Introduction

MCDONNELL Douglas has accumulated considerable background in the development and use of the "woven structure" concept, a fiberglass/polyimide sandwich structure in which the webs are woven integrally with the face sheets, eliminating unreinforced bondlines. The concept presently is employed in DC-10 airplanes as an acoustic inlet duct structure for the auxiliary power units (APU). The approach appears to be applicable as well to nacelle acoustic panels with potential for substantial reduction in cost and some reduction in weight. However, to assure that such a concept can be used to reduce cost or weight of an existing component, it must be shown that it can perform the same structural job as the existing component.

The purpose of the program described here is to subject a composite nacelle component to the real-life service environment of commercial airplane nacelles in a program leading to certification, and verify that the expected structural adequacy is indeed achievable for future production application. The component selected was an acoustic panel in the inlet nose cowl of a DC-10 wing engine. The present acoustic inner "barrel" of the DC-10 wing engine nose cowl is composed of three 120° panels made of perforated aluminum sheet on the inside and solid aluminum sheet on the outside, both bonded to an aluminum honeycomb core, to form an acoustic sandwich.

Figure 1 shows the location selected for the prototype composite panel. The lower panel position was selected because it presented the most severe problem from the standpoint of exposure to the environment and to service maintenance conditions. It is subjected to sunlight, settling dust and moisture, and service personnel walking on it, as discussed in the following.

Airframe and Mission Structural Requirements

The nose cowl acoustic inner barrel (Fig. 1) is a secondary structure carrying the nose cowl aerodynamic and inertia loads from the outer cowl fairing to the acoustic barrel and, thence, aft to the engine front face. The loads are transferred to the engine via a limited number of fittings with attach bolts to facilitate removal and replacement of the nose cowl in commercial operations.

The sound pressure level at the front face of the CF6 engine is of the order of 165 dB. The ability of the polyimide/fiberglass material to maintain structural integrity

in the intense sonic fatigue environment was a matter of concern, and the acoustic face of the sandwich was designed with that in mind.

It is normal service procedure to gain access to the engine fan by simply walking into the inlet. Inspectors therefore can be expected to be walking on the bottom panel to inspect the acoustic material and the engine fan blades. Mechanics can repair blades or replace them, gaining access in the same manner. This exposes the inlet acoustic barrel to the "handling" loads that can be imposed under such circumstances. Tools may be dropped on the bottom panel, or engine components, such as fan blades, may accidentally strike the surface.

During icing conditions, or on occasions when the nose cowl anti-ice valve is failed in the open position, hot compressor discharge air is ducted to the leading edge of the nose cowl. From the leading edge it is dumped into the annular chamber between the inner acoustic barrel and the outer nose cowl fairing. This exposes the acoustic panels to temperatures of the order of 450°F under the worst conditions (120°F day sea-level takeoff). The reason that the anti-ice valve could be open under such conditions is that the airplane is dispatchable with the valve failed or locked open. Where scheduling does not permit repair or replacement of the valve, an airline operator may therefore continue to use an airplane for a limited time with the anti-ice valve open. Polyimide was used as the resin system in order to retain structural integrity under the conditions just discussed.

Design

The basic sandwich construction is shown in Fig. 2. It consists of a basic x-core and four plies of commonly used glass fabric co-cured to the x-core. For acoustic absorption, the webs were designed to have a porosity of 20 cgs rayls at 20 cps approach velocity and the face sheet, 10 cgs rayls. The cgs rayls are simply pressure drop coefficients across the material

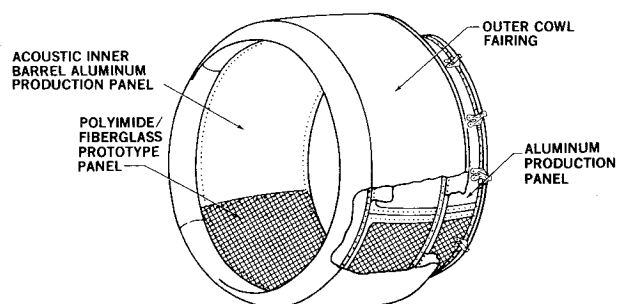


Fig. 1 DC-10 nose cowl assembly.

Presented as Paper 76-734 at the AIAA/SAE 12th Propulsion Conference, Palo Alto, Calif., July 26-29, 1976; submitted Aug. 9, 1976; revision received Jan. 18, 1977.

Index categories: Noise; Powerplant Design; Structural Materials.

*Senior Engineer/Scientist.

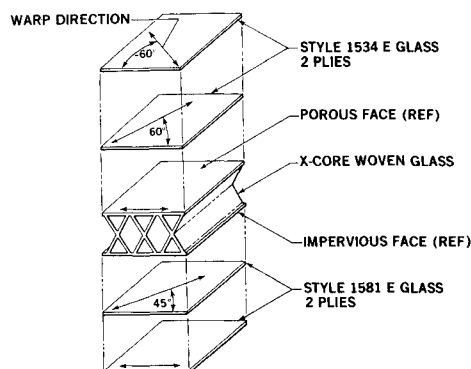


Fig. 2 Sandwich construction.

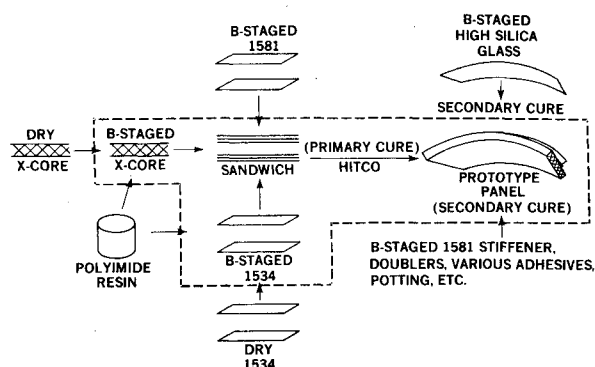


Fig. 3 Prototype panel fabrication.

with the approach velocity expressed in centimeters per second and the ΔP in dynes per square centimeter.

The back face of the sandwich is impermeable and is designed for static loading and pressure retention. Therefore, the style 1581 weave is used. It is an 8-harness satin which is dense for impermeability and compliant for fabricability. It is possible to achieve a porous acoustic face by integrally weaving two or more plies with the core. However, tests of such a configuration in an acoustic fatigue facility indicated weakness in the warp direction. This was verified by tensile tests of the acoustic face sheet material. It was concluded that the weakness could be due to the extreme variations in degree of prebuckle in the face sheet yarns because of the interlocking nature of the weave. A more uniform prebuckle was achieved by the use of the style 1534 weave, which is an open plain weave. Furthermore, since the lead time for loom setup to weave the core was a matter of several months, the use of co-cured plies of off-the-shelf fabrics afforded the opportunity to experiment in the meantime with tensile specimens and rayl tests of the face sheet materials. This assured meeting the design requirements when the core material became available.

The fore-and-aft and forward edge closeouts were tapered to flanges parallel to the wetted surface. The core material was scarfed to avoid concentration of stresses and to provide for ease in panel assembly. The flanges were made of a number of doubler plies of style 1581 glass fabric bonded to the basic sandwich with a secondary cure. The aft closeout was a potted joint utilizing a high-temperature potting compound, with doublers as required to take the bearing loads of the fasteners.

Eleven inches forward of the aft edge of the panel is a T-section stiffener which attaches to the nose cowl closing bulkhead. The aft 11 in. are part of the nacelle accessory compartment boundary and, as such, must provide fire barrier capability. To satisfy that requirement, one ply of style 1575 high-silica glass fabric was bonded to the back in that area.

Fabrication and Installation

A flow chart of the prototype panel fabrication process is shown in Fig. 3. A number of triangle- and diamond-shaped aluminum mandrel sets were used for preliminary checks of the specimens produced. It was found, however, that a good evaluation of the fit between the weave and the mandrels could be made only by curing an impregnated panel and cutting it open to permit inspection of the resulting core structure.

Adjustments of the loom were continued until a contoured panel was cured which met the specification requirements. The decision then was made to proceed with the prototype panel and the 60 ft² of flat panel for mechanical properties tests. The sequence of steps in the fabrication of the prototype panel is illustrated in Figs. 4-6. All curing was done at atmospheric pressure with a vacuum bag. The lower production

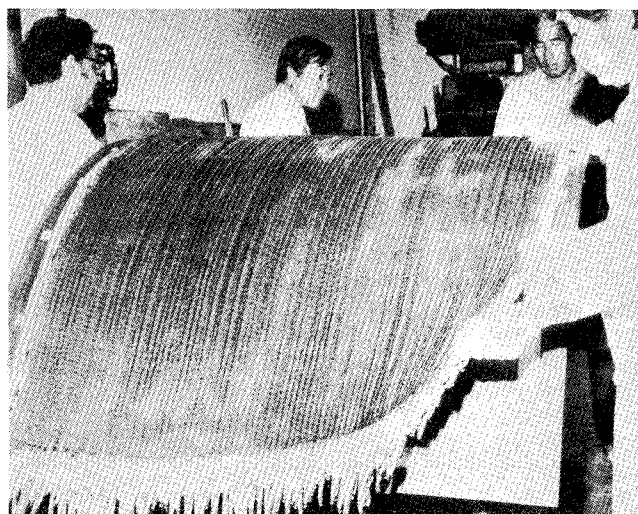


Fig. 4 B-staged x-core being assembled on porous face-ply.

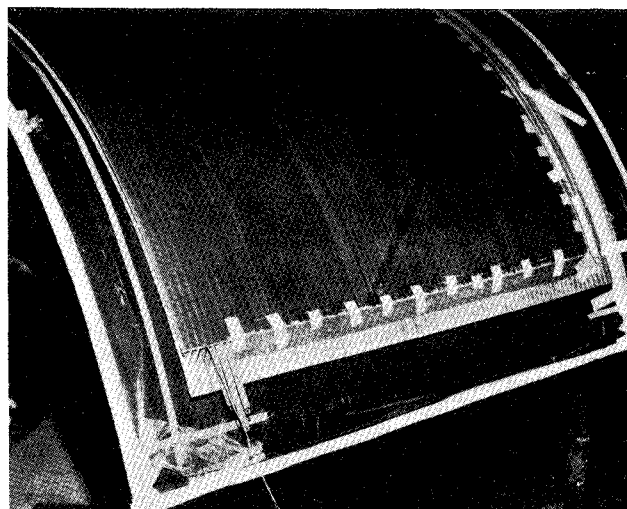


Fig. 5 Panel prior to assembly of edge doublers.

panel was removed from a spare flight test nose cowl and the prototype polyimide/fiberglass panel was installed in its place. The installation proceeded with very little trimming required.

Mechanical Properties

Aft Joint Tensile Test

The aft closure of the panel transmits the nose cowl inertia and aerodynamic loads to the engine forward flange. The load path goes through a number of fittings which are attached to the engine flange, to facilitate installation and removal of the

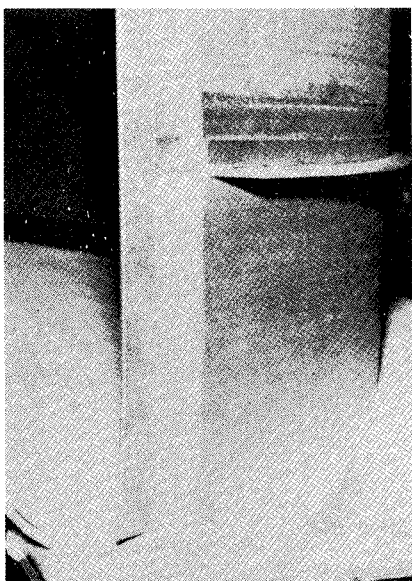


Fig. 6 Fabrication complete.

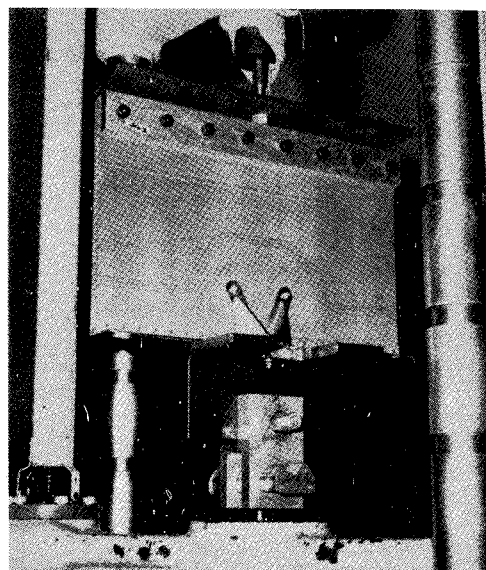


Fig. 8 Aft joint test setup.

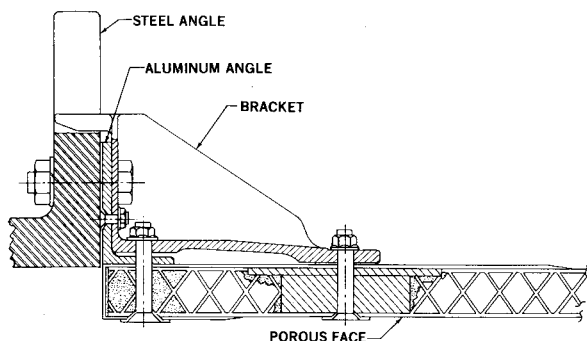


Fig. 7 Prototype aft joint specimen section.

nose cowl in service. Figures 7 and 8 show the test setup. The panel was loaded at a rate of 0.05 in./min and went to 23% above the design ultimate load, at which point the attach bolt failed. The basic panel itself retained its structural integrity, though the fire shield material (high-silica glass fabric) failed in the vicinity of the hard points to which the bracket was attached.

Design-Allowable Stresses

The inlet barrel is considered to be secondary structure and, as such, it is designed to "B" allowable stresses.¹

Program

As part of the planning of the polyglass panel development, a complete schedule of mechanical properties tests was prepared, covering tests deemed necessary to assure structural integrity and acceptance by the FAA of panel certifiability. Only those tests which were considered necessary to gain confidence in the material's structural integrity prior to the flight tests were conducted at this time. Ten specimens were used in each type of test to obtain reasonable confidence in the results.

The aft closure of the panel is the most highly loaded because the overhanging moments of the nose cowl are the highest in that area. The edgewise compression and face sheet tensile tests therefore were considered rather basic, and the performance of the tests were considered desirable prior to flight testing. Core shear tests in the transverse direction were felt to be necessary because face sheet loads will be carried from the inside face to the outside face via the core, in the transverse shear mode, at the forward joint.

Test Setup

The testing machines and instruments were checked and calibrated prior to the tests by a certified vendor's representative. Extensometers were used to measure deflections and the load-deflection curve was plotted for each test. However, in the case of the tensile tests, the extensometer always was removed prior to failure, in order to avoid damage to the instrument.

Test Results

Figure 9 illustrates typical edgewise compression failures. Figure 10 shows two stages of core shear strain, past the stability point. The left-hand view of Fig. 10 indicates the mechanism of buckling as it starts. When testing this particular specimen, it was decided to extend the strain to a very severe degree to determine the effect on the webs. The right-hand part of Fig. 10 shows the specimen still under load and with the extensometer removed. It should be emphasized here that, even after the extreme strain shown, little permanent set remained after release of the load. The core returned to what visually appeared to be its original configuration when the load was removed. The results of the face sheet tensile tests are shown in Figs. 11 and 12. As may be noted from Fig. 12, the impervious face had more of a tendency to make a clean break than the porous face, and the break was characteristically at the joint where the webs connect to the face sheet.

A summary of the test results is shown in Table 1. Figure 13 illustrates the degree of variation of the data, plotted as \pm one standard deviation about the average, which is represented as 100%. Figure 14 shows the approximate proportionality between face sheet strength and modulus. This indicates a good balance between the porous inner face and the impervious outer face, in that they both will fail at approximately the same strain.

Blade Fragment Penetration Resistance

There have been occasions where ingestion of foreign objects into the engine, such as large birds, has caused fan fragments to be ejected forward and impinge on the inlet acoustic panels. It was considered necessary, therefore, to verify that the polyimide/fiberglass acoustic panel structure was at least as penetration resistant as existing production panels. Figure 15 shows a comparison of tests results comparing polyimide acoustic panels with Stressskin (a resistance welded stainless acoustic panel with honeycomb core) and with sheets of 7075-T6 aluminum.

Fig. 9 Edgewise compression tests.

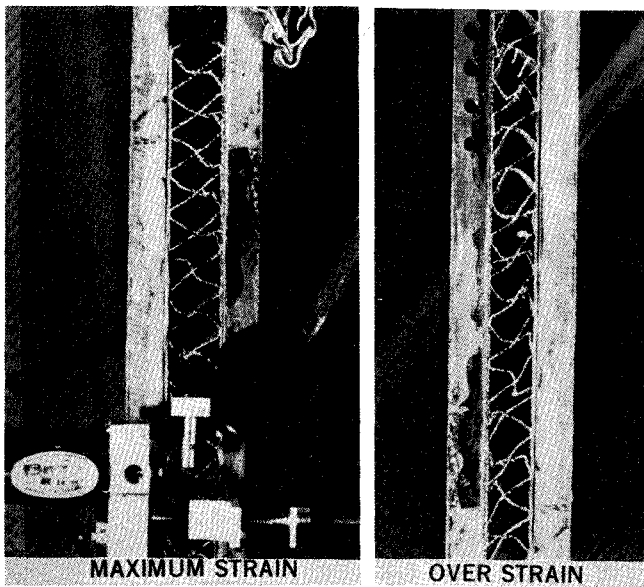
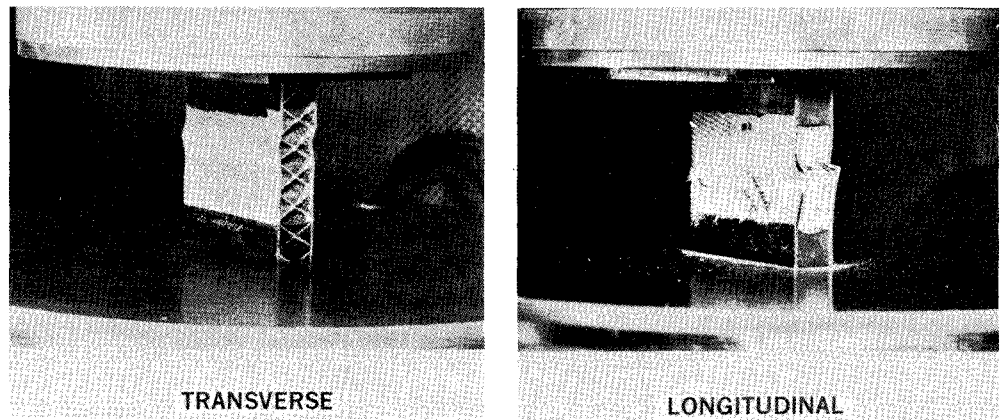


Fig. 10 Core shear test.

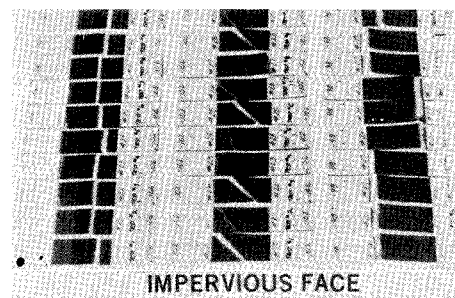
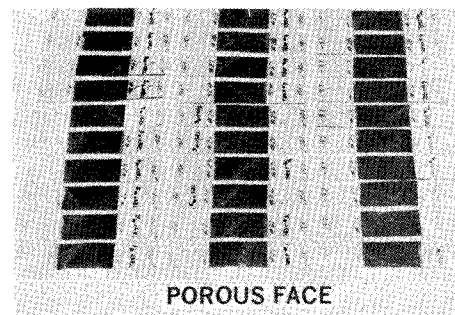


Fig. 12 Face sheet tensile specimens after test.

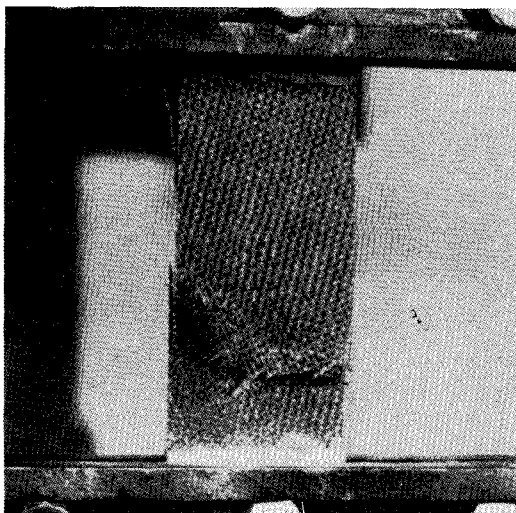


Fig. 11 Typical porous face sheet tensile test.

The correlation method² is as follows:

$$E = L\tau t^2 / \cos^2 \theta$$

where

E = energy absorbed by penetration

L = periphery of the projected surface of the fragment

τ = dynamic shear strength of target material

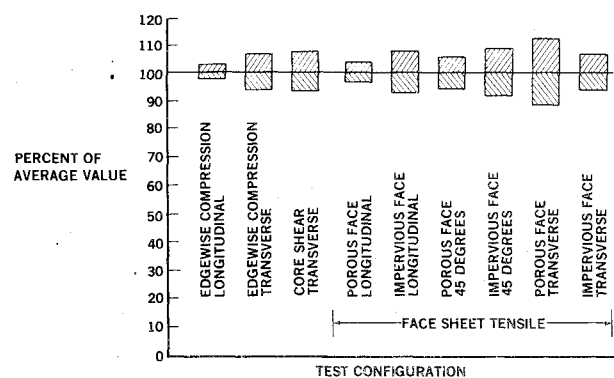


Fig. 13 Data scatter - standard deviation.

t = thickness of target

θ = angle between the trajectory and normal to the target

The dynamic shear strength τ is in reality a coefficient for a given type of material, which is determined by testing. Since the type of material and the thickness determine the panel area density (psf), it is possible to plot the specific energy- (E/L) against area density for a particular type of structure. This provides a convenient method of assessing the relative merit of different materials or types of construction based on weight.

Table 1 Mechanical properties test results

TEST	WEB ANGLE (DEGREE)	PARAMETER	AVERAGE VALUE	"B" ALLOWABLE	AVERAGE MODULUS (PSI)
EDGEWISE COMPRESSION	0	P_{CR} — LB/IN.	1159	1060	
	90	P_{CR} — LB/IN.	523	450	
CORE SHEAR	90	F_{su} — PSI	116.5	96.7	G/10 ³ 33.4
FACE SHEET TENSILE					
	POROUS	F_{tu} — PSI	14,380	13,200	E/10 ⁴ 1.44
	IMPERVIOUS	F_{tu} — PSI	25,358	20,700	2.27
	POROUS	F_{tu} — PSI	15,084	12,900	1.41
	IMPERVIOUS	F_{tu} — PSI	21,948	17,500	1.91
	POROUS	F_{tu} — PSI	13,715	9,750	1.28
	IMPERVIOUS	F_{tu} — PSI	18,577	16,000	2.13

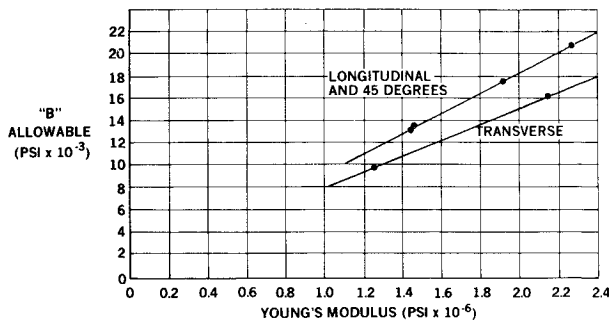


Fig. 14 Face sheet tensile strength vs modulus.

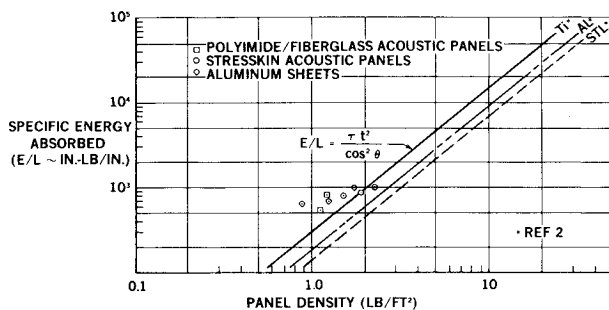


Fig. 15 Blade fragment penetration energy.

The target specimens were 10-12-in. square, mounted in a rigid frame to eliminate any effect of energy absorbed by resilience of the mounting structure. The simulated blade fragment in each case was a rectangular piece of titanium plate $3 \times 5 \times 0.230$ in. fired from a large air-gun utilizing a polyethylene sabot. The sabot was caught by a sabot stripper at the muzzle. All of the shots discussed here were made at an angle of incidence of 90° (normal to the target surface) with the short edge of the projectile forward to obtain comparable results. The velocity into the target was measured by electrical signals from grounding circuits at the gun muzzle. The velocity of the projectile after passing through the target was measured by electrical signals produced by breaking of carbon rods. The necessary approach velocity to assure penetration was estimated before the tests, since tests in which the simulated fragment does not penetrate, do not yield any numerical information.

Bonded aluminum honeycomb panels were not available at the time of the testing. Nevertheless, Stresskin is used in some inlet applications, so the comparison is considered to be of value. It should be emphasized, however, that the foregoing comparison may not be valid for other materials or sandwich configurations.

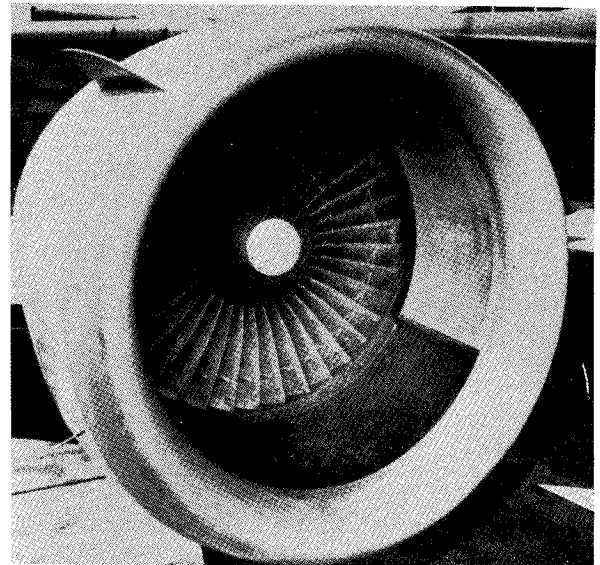


Fig. 16 Prototype panel on DC-10 flight test airplane.

Ground and Flight Tests

Since the inlet panels are in front of the engine, it was considered necessary to compile at least 5 hr of high-power time on the ground in order to establish sufficient confidence in the panel's structural integrity prior to flying it in the DC-10 flight test airplane. Arrangements were made, therefore, to test the nose cowl with the polyimide/fiberglass panel installed on the inlet of a CF6-50 engine which was scheduled to undergo cycle testing. The panel was exposed to 231 C-cycles while on the inlet of a CF6-50 engine. The total time was 56.4 hr, of which 20.8 hr were at 90% N_1 and above, and 9.3 hr were at takeoff thrust. The panel was inspected at intervals during the tests and at completion. No evidence of failure was detected at any time.

On completion of the ground tests, the nose cowl was installed on the DC-10 flight test airplane in the No. 3 engine position, Fig. 16. The panel subsequently has been exposed to all scheduled flight test operations. On two flights the anti-ice valve was left open on takeoff to determine any effects of the high temperature on the panel. It was expected that any effects of differential thermal expansion would be observable at the fasteners near the forward corners of the panel. After the anti-icing flights, the panel and fasteners were inspected carefully. No sign of distress whatever was observed.

At the present time, 288 flight hours have been accumulated with no sign of deterioration. The initial inspection schedule required complete inspections after each flight. This now has been relaxed to a "walkaround" inspection after flights and a complete inspection every 24 flight hours. The serviceability of the material was discussed with operating personnel of a number of the major airlines. No important operating problems or objections to the use of the material were revealed by the discussions.

Weight and Cost

At the time the prototype panel was installed in the nose cowl, both it and the replaced aluminum production panel were weighted on the same certified scales. The fiberglass/polyimide prototype panel showed a 12% weight advantage. In order to obtain a cost comparison, detailed back-to-back cost estimates were made by the same production estimators of both the fiberglass/polyimide and aluminum panels. Based on 300 ship sets and a production design in both cases, the fiberglass/polyimide showed approximately a 30% cost reduction compared to current production of aluminum panels, and 40% reduction com-

pared to a new design of the aluminum panel, in which start-up costs would be included.

Conclusions

Based on the work performed to date, the following conclusions can be drawn with respect to the prototype panel.

1) Feasibility of fabrication is assured of a flightworthy panel mechanically interchangeable with the production panel.

2) The mechanical properties are adequate, based on initial mechanical testing.

3) The panel has shown no degradation during ground and flight testing to date.

4) The polyimide/fiberglass panel structure is equal to the Stresskin production acoustic panel from the standpoint of blade fragment penetration resistance.

References

¹"Metallic Materials and Elements for Aerospace Vehicle Structures," Military Standardization Handbook MIL-HDBK-5B Sept. 1971.

²Vowles, D. F. and Coombs, T. W., "Structural Effects of Engine Burst Noncontainment," British Aircraft Corporation, Ltd. Rept. No. SST/B44-TWC/0113, March 1974.

From the AIAA Progress in Astronautics and Aeronautics Series . . .

INSTRUMENTATION FOR AIRBREATHING PROPULSION—v. 34

Edited by Allen Fuhs, Naval Postgraduate School, and Marshall Kingery, Arnold Engineering Development Center

This volume presents thirty-nine studies in advanced instrumentation for turbojet engines, covering measurement and monitoring of internal inlet flow, compressor internal aerodynamics, turbojet, ramjet, and composite combustors, turbines, propulsion controls, and engine condition monitoring. Includes applications of techniques of holography, laser velocimetry, Raman scattering, fluorescence, and ultrasonics, in addition to refinements of existing techniques.

Both inflight and research instrumentation requirements are considered in evaluating what to measure and how to measure it. Critical new parameters for engine controls must be measured with improved instrumentation. Inlet flow monitoring covers transducers, test requirements, dynamic distortion, and advanced instrumentation applications. Compressor studies examine both basic phenomena and dynamic flow, with special monitoring parameters.

Combustor applications review the state-of-the-art, proposing flowfield diagnosis and holography to monitor jets, nozzles, droplets, sprays, and particle combustion. Turbine monitoring, propulsion control sensing and pyrometry, and total engine condition monitoring, with cost factors, conclude the coverage.

547 pp. 6 x 9, illus. \$14.00 Mem. \$20.00 List

TO ORDER WRITE: Publications Dept., AIAA, 1290 Avenue of the Americas, New York, N. Y. 10019